Co-simulation of Circuit/Circuit type Solvers for EMC Applications Using a New Relaxation Method

Amadou Bayaghiou Diallo
Univ Lyon, Ecole Centrale de Lyon, INSA Lyon, Université Claude Bernard Lyon 1, Ampère, UMR CNRS 5005
Ecully, France
Amadou.Diallo@ec-lyon.fr

Christian Vollaire
Univ Lyon, Ecole Centrale de Lyon, INSA Lyon, Université Claude Bernard Lyon 1, Ampère, UMR CNRS 5005
Ecully, France
Christian.Vollaire@ec-lyon.fr

Arnaud Breard
Univ Lyon, Ecole Centrale de Lyon, INSA Lyon, Université Claude Bernard Lyon 1, Ampère, UMR CNRS 5005
Ecully, France
Arnaud.Breard@ec-lyon.fr

Mohamed Bensetti
GeePs – Group of electrical engineering - Paris, UMR CNRS 8507, CentraleSupélec, Université Paris-Saclay, Sorbonne Université, 3 & 11 rue Joliot-Curie, Plateau de Moulon 91192
Gif-sur-Yvette, France
Mohamed.Bensetti@centralesupelec.fr

Lionel Pichon
GeePs – Group of electrical engineering - Paris, UMR CNRS 8507, CentraleSupélec, Université Paris-Saclay, Sorbonne Université, 3 & 11 rue Joliot-Curie, Plateau de Moulon 91192
Gif-sur-Yvette, France
Lionel.Pichon@centralesupelec.fr

***Abstract*—This paper studies a new co-simulation scheme for coupled problems that is based on the principle of the adapted transmission line with an application to circuit-circuit type coupled simulations. *Co-simulation* between two or more circuit solvers is usually based on *waveform relaxation* methods and it results in an iterative process whose convergence depends on the type of *interface variables* (IVs) on the interface between the sub-circuits. The convergence of the IVs of this new method is tested in two examples of circuit simulations: a functional simulation of a Buck converter and an EMC simulation.**

***Index Terms*—Co-simulation, Waveform relaxation, Buck converter simulation, EMC simulation, Interface variable**

I. Introduction

The increasing number of static conversion devices (power electronics) in automobile systems and their growing impact on the on-board electronics and on the vehicle's electrical network involve severe constraints in terms of reliability and safety. Today, car and aircraft manufacturers are faced with two major concerns: On the one hand, they must ensure compliance with standards limiting parasitic emissions and the exposure of people to electromagnetic fields (EM) radiated inside the vehicle, and on the other hand, they must guarantee the proper functioning of all equipments in a normally polluted EM environment. The challenges in the vehicles for the future move beyond these aspects through the vulnerability to EM aggressions of the autonomous driving systems. Indeed, the cables and the inputs/outputs are inputs for disturbances aimed to dysfunction the guidance or to facilitate EM spy on the vehicle status. It is therefore essential to evaluate the levels of EM disturbances of these systems from the design phase. Although regular efforts to develop predictive models of electromagnetic disturbances [1]–[5], the measurement remains essential for complex embedded systems in the automotive industry. In addition, despite the improvement of system-oriented modeling and the computing power available over the last twenty years, the direct use of existing simulation tools (MATLAB, PSIM, SABER, CST Studio) for the analysis of a large system, considering all the strong interactions between subsystems, is an almost impossible mission. Several reasons can be given:

- In the automotive domain, where different industrial partners are involved, a multi-level analysis leads to multi-scale problems that are difficult to access by only one of the partners.
- A global simulation is very costly in terms of time and storage memory.
- The global numerical simulation of the system can only be carried out if all the models of the subsystems are known and available (different simulation platforms, evolution of the models in the development phases, confidentiality).

Co-simulation is in this context an approach that allows to bypass these different problems of complexity, confidentiality, storage memory and simulation time of these systems. With this methodology, each simulation tool deals with only one part of the system and each tool collaborates with all the others by exchanging certain variables that have been well chosen according to the system splitting, called interface variables (IVs). Waveform relaxation (WR) methods is a domain decomposition method for solving time-dependent problems, where two or more subproblems are solved independently for a certain time interval $[t_i, t_i + \Delta T]$ before exchanging the IVs. Iterations between the subproblems are performed over

978-1-7281-5579-1/20/$31.00 © 2022 IEEE

this interval until convergence, before moving to the next interval. WR methods have been proposed and used successfully since the 80's in circuit simulators like Spice [6], and more recently in electromagnetic field-circuit computation [7]. WR allows the implementation of co-simulation where each sub-problem (circuit-circuit or circuit-field) is respectively solved by their specialized solvers with an independent adaptation of the integration time step of each sub-problem. The major limitation of WR methods is the number of iterations required to reach convergence. On the one hand, keeping the number of iterations low is therefore crucial for the efficiency of the computation and on the other hand, convergence and its speed depend mainly on the choice of the IVs.

In this paper, we propose a new WR method applied to circuit-circuit co-simulation. This method is based on the principle of a matched transmission line that is virtually introduced at the splitting point. To implement the co-simulation, we assume that the simulators are black boxes and that the only information available at the interface are the IVs in each subsystem. This paper is structured as follows: Section II reviews the main interface variables proposed in the literature, Section III introduces the new interface variable and the convergence of this method, Section VI presents the co-simulation results for the two test cases, and Section V concludes the paper.

II. Interface Variables For WR Methods

The interface variables also called boundary conditions in the literature represent the equivalent model used to replace one subsystem when simulating the other. The main approaches used in the literature for circuit-circuit or field-circuit co-simulation are summarized in Fig.1 and to simplify the representation, we only assume the coupling of two subsystems.

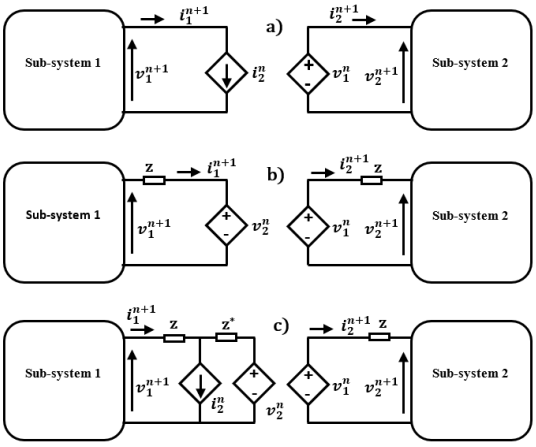

Fig. 1. Boundary conditions.

In the first scheme known as VI coupling, (Fig.1a), when simulating one sub system, the other is replaced by an ideal voltage or current source whose value is given by the previous iteration of the relaxation scheme [8]. This method is also widely used in the simulation with Hardware in the loop because it is easy to implement and it has a good accuracy. This method is unfortunately very unstable as shown in [9] [10], the impedance of subsystem 2 must be higher than the impedance of subsystem 1 at any time and at each iteration to guarantee a convergence of the method. Another approach, used for example in [6] and illustrated in (Fig.1b) is the voltage coupling. When simulating one sub-system, the other is replaced by a voltage source and vice versa. This method has very good stability for linear system but has poor accuracy. The last approach (Fig.1c) combines the advantage of the first two methods, namely the good stability of one and the accuracy of the other. Indeed, a judicious choice of Z^* allows to control the convergence without much affecting the accuracy of the result. This method is also known in the literature as the damping impedance method [11].

Besides the interface variables, it is also important to define how the data are exchanged during the co-simulation. The two best known algorithms for data exchange are the Gauss-Seidel and Jacobi methods [6] [12]. With the Gauss-Seidel method, the subsystems are evaluated in a sequential manner in each time interval $[t_i, t_i + \Delta T]$, i.e., the output of one subsystem

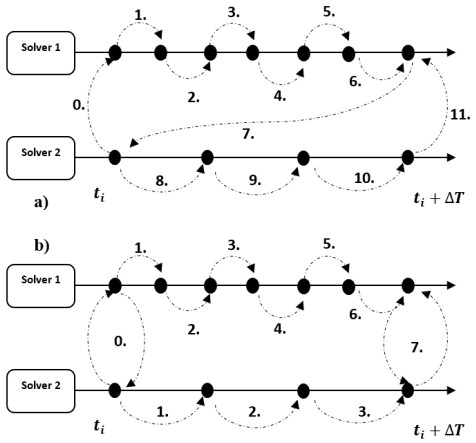

Fig. 2. Overview of orchestration algorithms; a - Gauss-Seidel Scheme and b - Jacobi scheme.

at time $t_i + \Delta T$ becomes the input of another at time t_i (Fig.2a). In contrast, for the Jacobi method, the subsystems are solved in parallel in a time interval $[t_i, t_i + \Delta T]$ using the inputs at time t_i (Fig.2b). The Gauss-Seidel method has the advantage of being more stable and accurate than the Jacobi method, but it is not desirable for co-simulating several complex subsystems because all the subsystems would have to be executed sequentially, which could lead to a very long computation time.

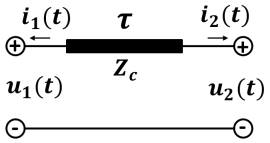

Fig. 3. Transmission line.

III. The Proposed Interface Variable

This new method is inspired by the behavior of transmission lines in electrical engineering, from which we derive the name Virtual Transmission Line (VTL).

A. Lossless Transmission line

A lossless transmission line can be modeled as an electrical circuit (Fig.3) which has a very particular behavior. When the transmission line is lossless and matched, the electrical voltage and current at the input line are the same as those at the output line with a delay τ. The electrical behavior of the lossless transmission line can be described by the equation (1).

$$\begin{cases} u_1(t) + Z_c i_1(t) = u_2(t-\tau) - Z_c i_2(t-\tau) \\ u_2(t) + Z_c i_2(t) = u_1(t-\tau) - Z_c i_1(t-\tau) \end{cases} \quad (1)$$

Where $u_1(t)$ and $i_1(t)$, represent the voltage and the outflow current of one side of the transmission line, while $u_2(t)$ and $i_2(t)$ represent those of the other side, Z_c is the characteristic impedance, t is the time variable and τ the propagation delay.

The idea of the new IV is to replace the propagation delay τ by the values of the previous iteration and the characteristic impedance Z_c by two impedances Z_{c1} and Z_{c2} which represent respectively the impedance of the adjacent subsystem at the splitting point (see the equation below where n is the iteration index). Finally, our method has the advantage of converging faster than the impedance damping method [11] for complex or non-linear subsystems in our case.

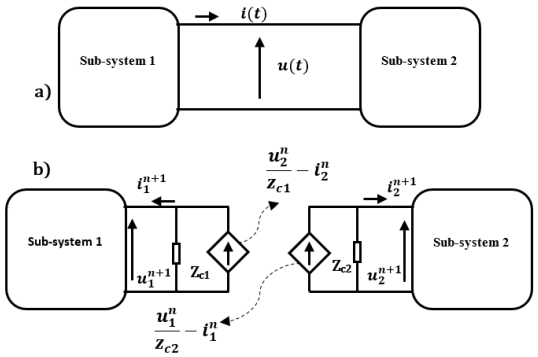

Fig. 4. a-Global system; b-subsystems with their Interface variables (IVs).

$$\begin{cases} u_1^{n+1}(t) + Z_{c1} i_1^{n+1}(t) = u_2^n(t) - Z_{c2} i_2^n(t) \\ u_2^{n+1}(t) + Z_{c2} i_2^{n+1}(t) = u_1^n(t) - Z_{c1} i_1^n(t) \end{cases} \quad (2)$$

B. Convergence Rate

For waveform relaxation methods, the determination of the convergence rate is equivalent to finding the spectral radius of the iteration matrix by deactivating all independent sources (Fig.4b) and by assuming that for each subsystem the equivalent impedance seen from the interfaces varies as a function of frequency. Kirchhoff's laws in harmonic regime at the interface (Fig.4b) give the equations (3).

$$\begin{cases} U_1^{n+1} - Z_1 I_1^{n+1} = 0 \\ -I_1^{n+1} + \dfrac{U_2^n}{Z_{c1}} - I_2^n - \dfrac{U_1^{n+1}}{Z_{c1}} = 0 \\ U_2^{n+1} - Z_2 I_2^{n+1} = 0 \\ -I_2^{n+1} + \dfrac{U_1^n}{Z_{c2}} - I_1^n - \dfrac{U_2^{n+1}}{Z_{c2}} = 0 \end{cases} \quad (3)$$

The capital letters represent the voltages and currents in frequency domain, while Z_{c1} and Z_{c2} represent the impedances of both sides (Thevenin impedances). In another way, Z_{c1} represents the impedance of subsystem 2 seen from the interface and Z_{c2} the impedance of subsystem 1 seen from the interface. The iteration matrix is given by (4).

$$\begin{pmatrix} I_1^{n+1} \\ I_2^{n+1} \end{pmatrix} = \begin{pmatrix} 0 & \dfrac{Z_{c1} - Z_2}{Z_1 - Z_{c1}} \\ \dfrac{Z_{c2} - Z_1}{Z_2 - Z_{c2}} & 0 \end{pmatrix} \begin{pmatrix} I_1^n \\ I_2^n \end{pmatrix} \quad (4)$$

The spectral radius of the iteration matrix is found as follows (5):

$$\rho = \left| \frac{Z_{c1} - Z_2}{Z_1 - Z_{c1}} \times \frac{Z_{c2} - Z_1}{Z_2 - Z_{c2}} \right| \quad (5)$$

To ensure the convergence of the iteration process, the maximum of the spectral radius must be less than 1. Because of the variation of Z_1 and Z_2 with frequency, the most obvious choice to keep the convergence rate below 1 is to take Z_{c2} = Z_1 or Z_{c1} = Z_2 and in this case, the convergence rate is zero and the number of iterations is usually less than 3. But unfortunately, it is difficult to find the impedance of each subsystem because of the confidentiality required for each subsystem. So, a way to approximate these impedances must be found to keep the convergence rate below 1 and to have a reasonable number of iterations.

C. Impedance approximation

To approximate each impedance Z_{c1} and Z_{c2}, we assume these impedances at the interface are resistive, which leads to 3 cases:

1st case: a default choice of these impedance values (for example 1 Ω). This IV method is known as VTL1.

2nd case: the impedances are approximated by the equations (Ohms' law at the interfaces) below and assuming that we are at convergence. This IV method is known as VTL2.

$$\begin{cases} u_1^{n+1}(t) = Z_1 i_1^{n+1}(t) \ \ \& \ \ u_1^n(t) = Z_1 i_1^n(t) \\ u_2^{n+1}(t) = Z_2 i_2^{n+1}(t) \ \ \& \ \ u_2^n(t) = Z_2 i_2^n(t) \\ Z_{c2} = \dfrac{u_1^{n+1}(t) - u_1^n(t)}{i_1^{n+1}(t) - i_1^n(t)} \\ Z_{c1} = \dfrac{u_2^{n+1}(t) - u_2^n(t)}{i_2^{n+1}(t) - i_2^n(t)} \end{cases} \quad (6)$$

The impedances are approximated by the RMS values of these impedances calculated previously Z_{c1} and Z_{c2} (6).

3rd case: it is assumed that the impedance of each subsystem

seen from the co-simulation interface can be easily and accurately evaluated at the maximum operating frequency of the global system. This IV method is known as VTL3.

IV. Application

The test case used to validate this new method is a Buck converter (Fig.5a) composed of a 9 Volts DC voltage source [13], two LISN (line impedance stabilization network) for the measurement of conducted disturbances, a DC-DC converter and the resistive load composed of ten resistors of 15 Ω in parallel. The whole test bench was modeled by an equivalent electrical circuit and solve with a circuit software. The global model allowing to extract the conducted disturbances of the differential mode is represented in Fig.5b. All the parasitic elements of the decoupling capacitors, the inductance, the LISN and the load were obtained by measurement with an impedance analyzer. For the active components (MOSFET and the diode), we used the models available in the LTSpice library to extract the important parameters. To validate the co-simulation, we used the Simscape® library from Simulink® to simulate each subsystem and MATLAB to manage the synchronization and information's exchange between the subsystems. All models were run on an Intel(R) Core (TM) i7-8665U CPU@1.90 2.11 GHz laptop. All solvers use a fixed time step to avoid the numerical oscillation of variable time step methods like the trapezoidal method.

A. Functional Simulation

The first validation is a functional co-simulation of the Buck converter (Fig.5b) without the parasitic elements at the switching frequency of 2.4 kHz to show the ripples at the output of the converter. The whole circuit is split in two parts at the interface between the converter and the load (Fig.5.c). For the three methods (VTL1,2,3), we set a maximum absolute value tolerance between $i_1^{n+1}(t)$ and $i_2^{n+1}(t)$ (see Fig.4b) less than 10^{-6} A and we launch the co-simulation until convergence. Fig.6 shows the time domain variation of the voltage and current in each sub-circuit compared to the reference simulation. It should be noted that before splitting the global circuit (Fig.5b), it is the same current that crosses the two subsystems and the same voltage applied at the splitting point.

To validate the assumption of approximating of the equivalent impedances (subsection III-C), we performed Fourier transform from 1 kHz to 1 MHz of the time domain electrical quantities (Fig.7) to see the impact of this approximation on the simulation result. From 1.0 kHz to 100 kHz, the currents and voltages of the co-simulation overlap with the reference simulation. From 100 kHz a small difference can be observe, but it is less than the tolerance 10^{-6}A set between the current in subsystem 1 and 2. However, as will be shown later, this approximation can introduce errors for high frequencies because if at 1 MHz the load is almost purely resistive, from 30 MHz, the load begins to have an inductive behavior. To minimize this error in high frequencies, we must choose a very low tolerance or a high number of iterations for the convergence criterion. To compare the performance of the three methods (VTL1,2,3), we set two criteria for stopping the iteration process. The first criterion is the tolerance $max|i_1^{n+1}(t) - i_2^{n+1}(t)| \leq Tol$ between the currents in subsystems 1 and 2 and a second criterion which is the maximum of iteration 10.

Fig.8 shows a slow convergence for the VTL1 method compared to the others due to a choice of default characteristic impedances of 1 Ω which is different from the impedance of the load at the switching frequency (1.5 Ω). It takes 4 iterations for the VTL2 method to converge while for the VTL3 method it takes only 2 iterations. Indeed, VTL3 uses the true impedance (1.5 Ω for the load) from the beginning of the co-simulation calculated directly at the switching frequency or at the maximum frequency. VTL2 method starts the simulation with false impedance values (1 Ω), the impedance is then approximate using equations (6).

B. EMC Simulation

The second validation is an EMC co-simulation of the Buck converter (Fig.5c) with the parasitic elements of the decoupling capacitors, inductor, and the resistive load up to 30 MHz. The switching frequency is 200 kHz. The co-simulation scenario for the EMC validation is the same as the one previously validated for the functional simulation. An EMC test bench was used to measure the conducted disturbances. The topology of this test bench was inspired by the CISPR25 standard [14] and is described in Fig.5a. A spectrum analyzer is used to measure conducted disturbances through the LISN. The Buck converter is the divice under test (DUT), located above a ground plane. The EMC co-simulation results in frequency domain (Fig.10b) are compared with the experimental spectrum. As shown in Fig.10b, there is good agreement between the measurement and both simulation types (reference and co-simulation) up to 30 MHz.

TABLE I
Co-simulation vs Reference In Frequency Domain

Freq (Hz)	Current (mA)			Voltage (mV)		
	SS1	***SS2***	***Ref***	***SS1***	***SS2***	***Ref***
0	2832.5	2832.5	2832.5	4192.1	4192.1	4192.1
200k	0.362	0.362	0.362	0.499	0.499	0.499
1M	0.058	0.058	0.058	0.081	0.081	0.081
10M	0.018	0.002	0.003	0.042	0.072	0.045
20M	0.036	0.005	0.006	0.092	0.089	0.103

To show the impact of the approximation of the impedances in high frequencies, we have calculated the Fast Fourier Transform of the voltage and current in the load (Table.I) with 20 iterations, where $SS1$, $SS2$ stands for subsystem 1 and subsystem 2 and Ref for reference. The error between the co-simulation and the reference for the mean value is less than 0.001% for the current and the voltage. From the switching frequency 200 kHz to 1 MHz, this error is also less than 0.001% and more than 5% at 1 MHz for the voltage in $SS1$ for example. Fig.9 shows the effect of this approximation, from 1 MHz where the inductive character of the load begins to appear, it takes more iterations to maintain the relative error below 10%. This may also be due to the amplitude of the

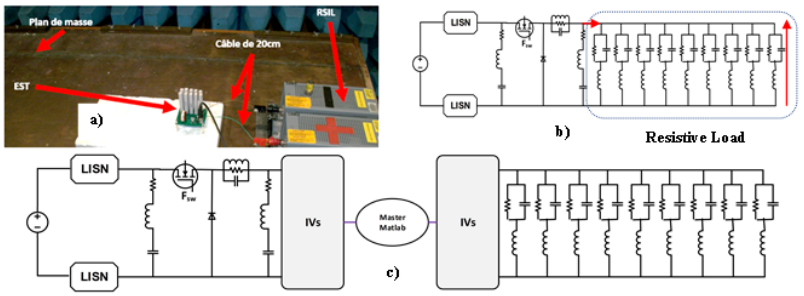

Fig. 5. Experimental Setup (a); Reference Electrical Model (b) Split Electrical Model for the co-simulation (b).

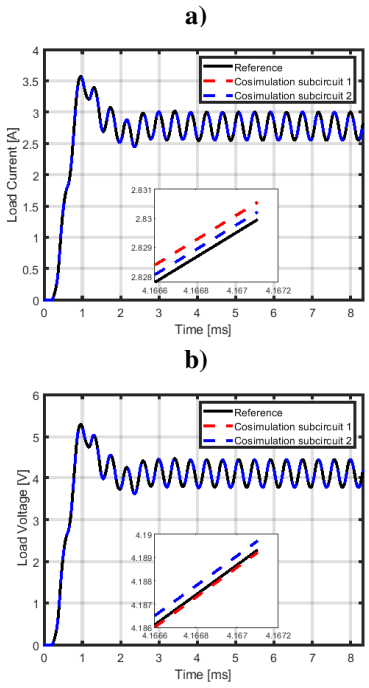

Fig. 6. Time domain trajectories of electrical quantities,Load current Reference vs Co-simulation (a); Load voltage Reference vs Co-simulation (b).

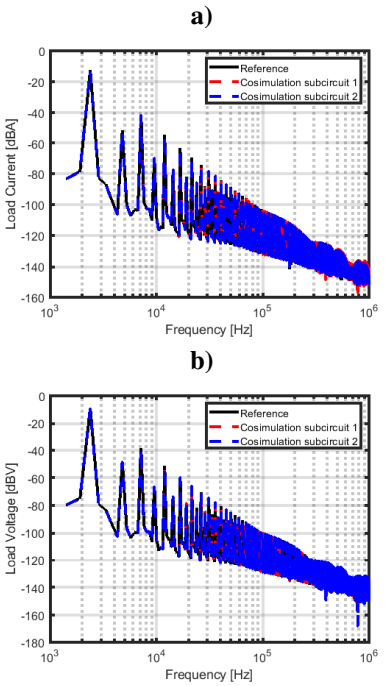

Fig. 7. Frequency domain of electrical quantities; Load current Reference vs Co-simulation (a), Load voltage Reference vs Co-simulation (b).

harmonics being very low compared to the tolerance for a given number of iterations. For example, after 20 iterations, the maximum relative error on the voltage in $SS1$ is less than 0.01% in the time domain but more than 5% from 10 MHz in frequency domain. It is therefore necessary to find a compromise between accuracy and simulation time which is not the subject of study in this paper.

Finally, we observe that the influence of the approximation of the characteristic impedance have not significant effects on the conducted disturbances (Fig.10b), because most of these disturbances are due to the switching between the MOSFET and the diode and the parasitic elements of the decoupling capacitors and the inductance. The subsystem 2, which is a resistive load, has small contributions to the high frequency disturbances.

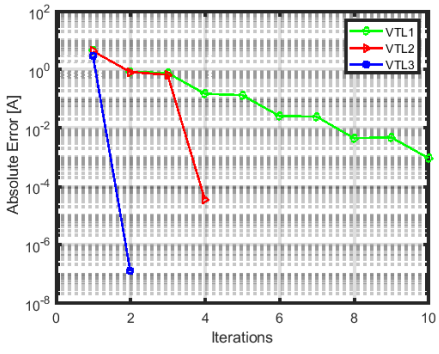

Fig. 8. Current absolute error between subsystem 1 and 2.

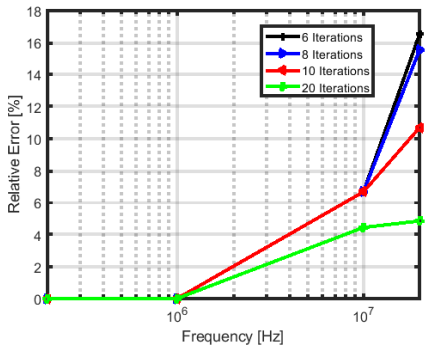

Fig. 9. Relative error for the load voltage in subsystem 1.

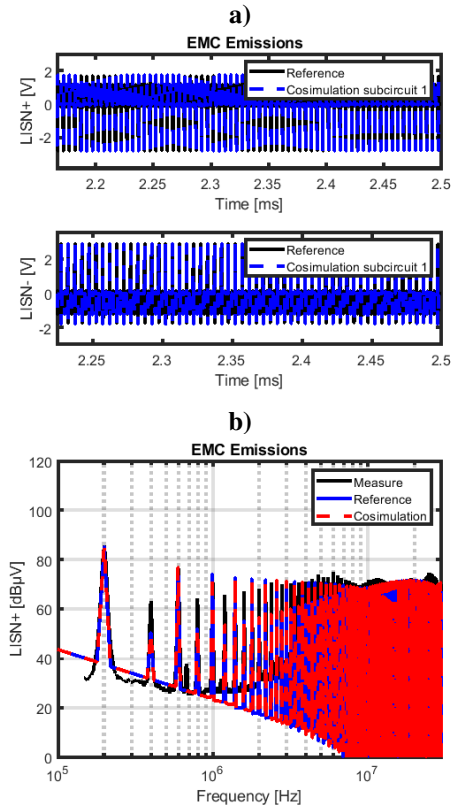

Fig. 10. EMC Emissions. Time domain (a) and Frequency domain (b), Reference versus co-simulation versus measurement.

V. Conclusion

This paper has presented and analyzed a new method for interface variables (IVs) for the simulation of coupled circuit-circuit type problems using WR waveform relaxation methods. Several variants of this method have been studied and have been successfully applied to two practical applications: Functional Co-simulation and EMC simulation of a Buck Converter.

Further applications of this new method will involve circuit solvers and electromagnetic solvers.

Acknowledgment

This research program is funded by the French National Research Agency (ANR): ECOCES project (Electromagnetic compatibility Co-simulation Of Complex Electrical Systems), ANR-19-CE05-0016-05.

References

[1] A. Gahfif, F. Costa, P.-E. Lévy, M. Berkani, B. Revol and M. Ali, "Conducted Noise Investigation for IMS Based GaN HEMT Power Module by Black Box Model," 2020 International Symposium on Electromagnetic Compatibility - EMC EUROPE, pp. 1-3, 2020.

[2] F. Costa, C. Vollaire and R. Meuret, "Modeling of conducted common mode perturbations in variable-speed drive systems," IEEE Transactions on Electromagnetic Compatibility, vol. 47, no. 4, pp. 1012-1021, 2005.

[3] M. Amara, C. Vollaire, M. Ali and F. Costa, "Black Box EMC Modeling of a Three Phase Inverter," 2018 International Symposium on Electromagnetic Compatibility (EMC EUROPE), pp. 642-647, 2018.

[4] M. Foissac, J.-L. Schanen and C. Vollaire, ""Black box" EMC model for power electronics converter," 2009 IEEE Energy Conversion Congress and Exposition, pp. 3609-3615, 2009.

[5] J. Liu, Y. Wang, D. Jiang and Q. Cao, "Fast prediction for conducted EMI in flyback converters," 2015 IEEE International Conference on Computational Electromagnetics, pp. 247-249, 2015.

[6] E. Lelarasmee, . A. E. Ruehli and A. L. Sangiovanni-Vincentelli, "The Waveform Relaxation Method for Time-Domain Analysis of Large Scale Integrated Circuits," IEEE Transactions on Computer-Aided Design of Integrated Circuits and Systems, vol. 1, no. 3, pp. 131-145, 1982.

[7] L. Yang, C. Yang, Y. Tu, X. Wang and Q. Wang, "Field-Circuit Co-Simulation Method for Electrostatic Discharge Investigation in Electronic Products," IEEE Access, vol. 9, pp. 33512-33521, 2021.

[8] X. Wu and A. Monti, "Methods for partitioning the system and performance evaluation in power-hardware-in-the-loop simulations. Part I," 31st Annual Conference of IEEE Industrial Electronics Society, 2005. IECON 2005., pp. 6 pp.-, 2005.

[9] V. Dmitriev-Zdorov, "Generalized coupling as a way to improve the convergence in relaxation-based solvers," Proceedings EURO-DAC '96. European Design Automation Conference with EURO-VHDL '96 and Exhibition, pp. 15-20, 1996.

[10] W. Ren, M. Steurer and T. L. Baldwin, "Improve the Stability and the Accuracy of Power Hardware-in-the-Loop Simulation by Selecting Appropriate Interface Algorithms," IEEE Transactions on Industry Applications, vol. 44, no. 4, pp. 1286-1294, 2008.

[11] A. Aguirre, M. Davila, P. Zuniga, F. Uribe and E. Barocio, "Improvement of damping impedance method for Power Hardware in the Loop simulations," 2016 IEEE International Autumn Meeting on Power, Electronics and Computing (ROPEC), pp. 1-6, 2016.

[12] M. Crow and M. Ilić, "The Waveform Relaxation method for systems of differential/algebraic equations," Mathematical and Computer Modelling, vol. 19, no. 12, pp. 67-84, 1994.

[13] M. Touré, F. Paladian, J. Taki, P.-É. Levy, M. Bensetti, F. Robert and L. Dufour, "Conducted EMI prediction using different levels of MOSFET models in a multi-physics optimizations context," 2016 International Conference on Electrical Sciences and Technologies in Maghreb (CISTEM), pp. 1-5, 2016.

[14] [Online]. Available: CISPR 25:2008 — IEC Webstore — electromagnetic compatibility, EMC, smart city, transportation, mobility.